Franck−Condon Modes in Sr_2MnWO_6 Double Perovskite

Yukari Fujioka,*,† Johannes Frantti,† and Masato Kakihana†,‡

Materials and Structures Laboratory, Tokyo Institute of Technology, Yokohama 226-8503, Japan, and Institute of Multidisciplinary Research for Advanced Materials, Tohoku University, Sendai 980-8577, Japan

Received: August 24, 2004

Molecules and color centers in crystals are known to exhibit a form of electron−phonon coupling, which is understandable by the Franck−Condon mechanism. In a Raman spectrum, this process is seen as a series of equidistant peaks whose relative intensities depend on the induced atomic vibration mode. The process has been predicted to be observable in crystals, but the difficulty in observing them has been related to the fact that the excited electron states tend to be delocalized. Correspondingly, it has been assumed that a self-trapping (localization) of the electron is necessary. Our polarization resonance Raman scattering data revealed two different series of Franck−Condon modes in double perovskite Sr_2MnWO_6 single crystals. One series corresponded to the Mn d orbital electron transition to the conduction band, whereas the second series corresponded to e_g to e_g transition (localized electron). The lattice distortion was estimated from the observed Franck−Condon peak positions and intensities.

The usual assumption done for the computation of atomic vibrations is called the Born−Oppenheimer approximation. It is based on the idea that light electrons can immediately follow the positions of heavy nuclei, making the computational task considerably easier. On the contrary, when electrons are excited to a very short-lived state, atomic nuclei cannot adjust their position within that time. It is only when the electronic excitation state has a lifetime comparable to the atomic vibration period that the nuclei can readjust their positions to achieve a new total energy minimum (lattice relaxation). The Franck−Condon principle applies to a case where light excites an electron from its ground state to a higher energy state with sufficiently long lifetime for a lattice relaxation.[1] The electric field of light can be treated as a perturbation within the framework of quantum mechanical perturbation theory. If the lattice distortion is sufficiently large, then this should result in a series of modes with energies $n\hbar\omega$ (n is positive integer, ω is the vibration frequency, and $\hbar$ is Planck's constant) seen as equidistant peaks in a Raman spectrum. Figure 1 gives the notation used in this study. The relative intensities of the peaks and their symmetry contain information from the lattice distortion and allow these peaks to be distinguished from peaks having different origins. Recently, Franck−Condon modes were theoretically predicted to be observable in $LaMnO_3$ via self-trapped excitons.[2,3]

We studied cubic double perovskite Sr_2MnWO_6 (SMW) single crystal (space group no. 225, $Fm\bar{3}m$) by polarized Raman scattering technique. The symmetry of the flux grown single crystal was confirmed by single-crystal X-ray diffraction measurements. In addition, data were collected on SMW powder at different temperatures between 80 and 733 K. The two types of B cations, Mn^{2+} and W^{6+}, are alternatively ordered along the crystal axes directions.[4,5] For the interpretation of Raman spectra, we note that SMW is paramagnetic down to 40 K.[5] This implies that collective excitations related to the spin ordering are unlikely above 40 K. Cubic SMW has four

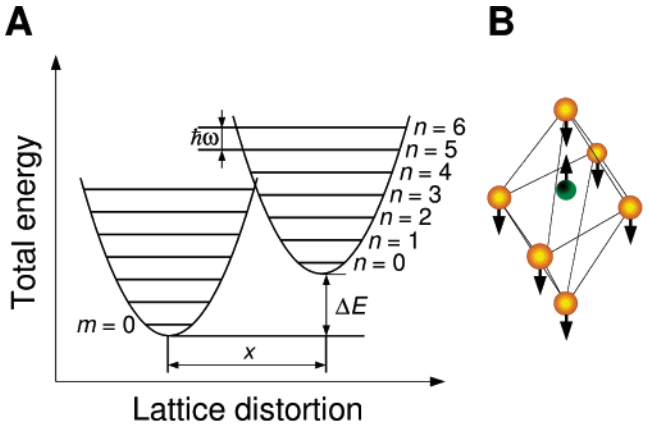

Figure 1. Schematic presentation of the Franck−Condon principle. (A) ΔE is the elastic energy, which is responsible for the total energy increase. x denotes the lattice distortion, which gives the displacement between the two harmonic oscillators. Also, the energy levels of the harmonic oscillators are shown. We considered only vibrational transitions between the ground state 0 and excited states n. (B) The oxygen octahedral distortion mode that follows the electron transition. Oxygen and manganese are presented by orange and green spheres, respectively. After electron transition, the vibrational quanta are excited, and the degeneracy splitting of the e_g orbitals follows this distortion.

Brillouin zone center Raman active lattice modes, two belonging to the T_{2g} symmetry, one to A_{1g}, and one to E_g symmetry mode. In the last two mentioned modes, only oxygen ions move. We used backscattering geometry where incoming light was coming perpendicularly to the (100) plane, light polarization direction was along the ⟨100⟩ direction (X direction), and the analyzer was either parallel (XX configuration) or perpendicular to the incoming polarization (XY configuration). XX configuration shows both the E_g and A_{1g} modes, wheras XY configuration reveals only the T_{2g} modes. To prevent decomposition of the SMW under the laser light, we kept the power below 150 μW. The laser beam spot size was 2 μm. Laser beam wavelengths were 457.935, 476.486, and 514.532 nm (Ar^+ laser) and 632.81646 nm (HeNe laser). By using different wavelengths,

* Corresponding author. E-mail: fujio2@msl.titech.ac.jp.
† Tokyo Institute of Technology.
‡ Tohoku University.

10.1021/jp046178f CCC: $27.50
Published on Web 10/09/2004

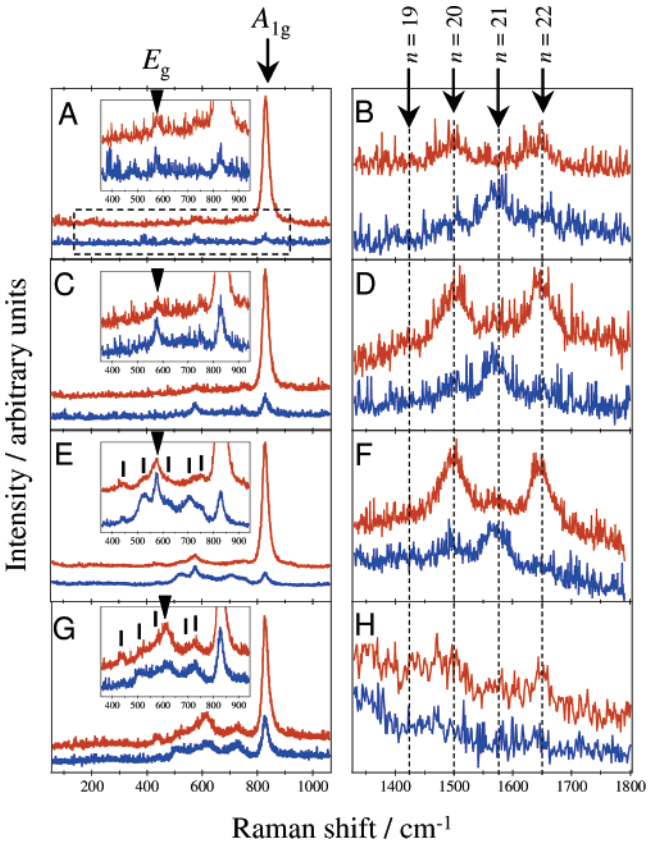

Figure 2. Raman spectra collected on SMW single crystal at room temperature using different laser beam wavelengths λ. Red and blue lines indicate spectra collected in *XX* and *XY* configurations, respectively. The box (- - -) in panel A indicates the range shown in insets in panels A, C, E, and G. (A and B) $\lambda = 457.935$ nm. (C and D) $\lambda = 476.48$ nm. (E and F) $\lambda = 514.532$ nm. (G and H) $\lambda = 632.81646$ nm. Only in the spectra shown in A and B, do the E_g and A_{1g} modes obey the selection rules given by the Raman tensors (which are valid for the nonresonance case). Peaks belonging to two series of modes, assigned to the Franck−Condon principle with different electron transitions, are indexed by letters *n* (process I) or were shown by tick marks (process II). Panels B, D, and F show the high-frequency series observed after short wavelengths were used, and panels E and G show the low-frequency series assigned to the e_g−e_g electron transition. Panels E and F correspond to the intermediate regime, where both types of Franck−Condon modes can be excited.

we could study the intensity dependence of the Raman spectra on excitation wavelength, confirm that the observed modes are truly Raman modes, and excite selectively different modes.

Figure 2 shows the Raman spectra obtained using different polarization geometries and wavelengths. The strong peak at 830 cm^{-1} is the totally symmetric A_{1g} mode, and the peak at 575 cm^{-1} is the E_g symmetry mode. The two T_{2g} modes had presumably too weak intensities to be observed. Figure 2B, D, and F show the high-frequency peaks observed at around 1425 (very weak, it is more clearly seen in Figure 3), 1500, 1575 and 1650 cm^{-1}, which are integer (*n*) multiples of 75 cm^{-1} (frequency of the fundamental vibration). The two strong peaks at 1500 ($n = 20$) and 1650 cm^{-1} ($n = 22$) appear in the *XX* configuration, whereas the two weaker modes at 1425 ($n = 19$) and 1575 cm^{-1} ($n = 21$) appear in the *XY* configuration. Totally symmetric modes tend to have the strongest intensity, which is also seen in lattice modes. Even overtones always involve the totally symmetric representation. Noting that the overtones of even (gerade) fundamental are always even and that the even and odd overtones of odd (ungerade) fundamental are even and odd, respectively, the consideration is limited to even fundamentals. The appearance of the $n = 21$ peak in the *XY* configuration hints that the odd overtone representation should contain the T_{2g} representation, which in turn implies that the fundamental vibration should belong to the T_{1g} or T_{2g} representation. For the case of nondegenerate fundamental vibration, the even overtone peaks belong to the totally symmetric representation, whereas odd overtone peaks belong to the same representation as the fundamental vibration.[6] However, the only Raman-active 1D representation is A_{1g}, which was ruled out (Figure 2). Other 1D representations do not have Raman-active odd overtones. Also, the doubly degenerate fundamentals are ruled out because their overtones would not be seen in the *XY* geometry. Because the origin of the frequency, symmetry, and temperature (shown below) dependence of all the modes is, in simplest terms, the same, we seeked a model explaining all of these features, assigned the peaks to the Franck−Condon mechanism, and further tested the model.

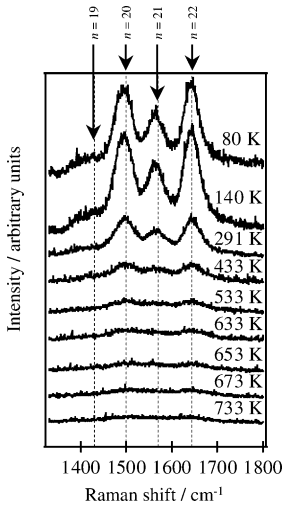

Figure 3. Temperature dependence of the Franck−Condon modes. Spectra were collected on SMW powder using a laser beam wavelength of 514.532 nm.

We estimated the band gap to be 2.5 eV (corresponds to the 497 nm) from the reflectance spectroscopy measurements carried out for the SMW powder. The electronic transition, corresponding to the spectra excited by 515-, 476-, and 458-nm laser light, was related to the electron transition from the Mn e_g orbital to the conduction band, that is, to a nonlocalized state (this Franck−Condon mode formation process was labeled as I). This explains why these modes are not observed once the laser light wavelength was 633 nm, Figure 2H. A Jahn−Teller-active Mn^{3+} ion is created in process I, which further enhances the lattice distortion. At longer wavelengths, Mn e_g to e_g electron transition becomes prominent, and another set of Franck−Condon modes are excited. This process (labeled as II) necessitates that the e_g orbital degeneracy is split, which is probable if the laser light creates Jahn−Teller-active Mn^{3+} ions. For the e_g to e_g transition to be allowed, their parities should be different. Because both scattering processes involve real electronic excitations (resonance case), the selection rules stated by the Raman tensors are not strictly obeyed; some intensity from the modes assigned to A_{1g} symmetry also appear in the *XY* polarization geometry. This was most apparent in spectra excited by long wavelength light.

To estimate the lattice distortion within harmonic approximation in case I, we assumed that Mn ion is shifted along the cube axis, whereas the surrounding oxygens move into the opposite direction (Figure 1B.) This vibration has an effective mass 25.62 u. Because of the lattice relaxation, the local symmetry

is decreased from the cubic one. This is consisted with the assumption that the e_g orbital degeneracy is split. The transition probability from the excited state n to the ground state is directly proportional to the product of squares of the electron transition probability (conventionally taken to be the same for both nuclei arrangements), state occupation probability,[7] and the Franck−Condon overlap integral. Although transitions between excited states are possible, their effect (within harmonic approximation) is to modify peak intensities, not their positions. The Franck−Condon overlap integrals can be estimated by assuming two harmonic potentials, whose minima spatial positions differ by an amount x (lattice distortion, as shown in Figure 1A). The force constant was adjusted so that the oxygen octahedra distortion mode (Figure 1B) would have an energy of 75 cm^{-1}. The overlap integrals of the displaced harmonic oscillator functions give the relative transition probabilities between initial state 0 and final state n. We adjusted the value of x so that the transition probability maximum occurred for $n = 20$, with slightly smaller probabilities for $n = 19$ and 21, which yielded a value of $x = 0.084$ Å. This value corresponds to the fast transition case[1] and is of the same order as the Mn thermal displacement amplitudes at room temperature. The study of the temperature dependence of these modes provides important insight to the phenomenon because it is thermal vibrations that finally wash away the Franck−Condon modes. One expects that the intensities of the Franck−Condon modes increase with decreasing temperature, although their positions have constant values (except the small frequency decrease due to the increase in bond lengths following the thermal expansion). The temperature dependence of these modes is shown in Figure 3. It is indeed seen that the peak intensities strongly decrease with increasing temperature and vanish together (supporting the idea that these peaks have common origin), although their positions are almost constant.

The peaks assigned to the process II were modeled in a similar manner, although the resonance conditions obscured the symmetry assignment. The peaks in this series were integer multiples of 44 cm^{-1}. The strongest peaks occurred for $n = 10$, 12, 14, 16, and 17, as indicated in Figure 2E and G. Using the same effective mass as above and adjusting x so that the transition probability maximum occurred for $n = 16$ led to the lattice distortion value $x = 0.076$ Å. We note that it is slightly smaller than the value obtained for process I, which is consistent with the fact that after electron excitation from the e_g orbital to the second e_g orbital electron is still localized. This process is similar to the creation of a localized polaron.

We note that, for process II, there were five overlapping peaks (in addition to the E_g and A_{1g} modes) with roughly equal intensities (with decent agreement with the model), whereas there were only four modes observed in the case of process I. The present model gave quantitative agreement with the observed peak positions for both processes. A quantitative model for peak intensities necessitates information from the nonequilibrium energy level populations and Raman scattering cross sections for different symmetry overtone modes. Thus, although the transition probabilities, as calculated from the Franck−Condon overlap integrals, follow Gaussian distribution, there is no reason to expect that the observed intensities would behave similarly.

We believe that the present experimental observations shed light on the currently active field of the orbital ordering, which has particularly been dedicated for $LaMnO_3$ materials.[2,3,8,9] The puzzling point in $LaMnO_3$ materials is that their magnetic ordering depends on stoichiometry.[10] This in turn obscures the orbiton wave interpretation. We hope that the two reported Franck−Condon processes in a paramagnetic system, differing in the nature of the electron excitations, help to understand the related phenomena in orbitally ordered systems; for instance, resonant Raman scattering experiments studying the possibility of creating Jahn−Teller-inactive Mn^{4+} ions and corresponding Franck−Condon modes by laser light should clarify the situation of $LaMnO_3$. We note that there indeed are four almost equidistant modes seen in the Raman spectra collected on $LaMnO_3$ single crystal (Figure 2d in ref 8).

Acknowledgment. We are grateful to Professor S. Sasaki (Tokyo Institute of Technology) for his valuable help in single-crystal X-ray diffraction measurements. Professors E. Yasuda and M. Yoshimura (Tokyo Institute of Technology) are acknowledged for supporting this study. J.F. is grateful to the Academy of Finland for financial support (project no. 201889).

References and Notes

(1) Harrison, W. A. *Solid State Theory*; Dover Publications: New York, 1980.
(2) Perebeinos, V.; Allen P. *Phys. Rev. Lett.* **1999**, *83*, 4828.
(3) Perebeinos, V.; Allen, P. *Phys. Rev. B* **2001**, *64*, 085118.
(4) Blasse, G. *J. Inorg. Nucl. Chem.* **1965**, *27*, 993.
(5) Azad, A. K.; Ivanov, S.; Eriksson, S.-G.; Rundlöf, H.; Eriksen, J.; Mathieu, R.; Svedlindh, P. *J. Magn. Magn. Mater.* **2001**, *237*, 124.
(6) Tinkham, M. *Group Theory and Quantum Mechanics*; Dover Publications: New York, 2003.
(7) The population of energy levels in thermal equilibrium is given by the Boltzmann factor. Time-resolved studies revealed that the excited state of molecules is relaxed within a picosecond scale, which is far too short of a time for thermal equilibrium, and the population of energy levels significantly deviates from the one given by Boltzmann factor. See, for example, Kasajima, T.; Akimoto, S.; Sato, S.; Yamazaki, I. *Chem. Phys. Lett.* **2003**, *375*, 227. Presumably, the relaxation times are of the same order in solids.
(8) Saitoh, E.; Okamoto, S.; Takahashi, K. T.; Tobe, K.; Yamamoto, K.; Kimura, T.; Ishihara, S.; Maekawa, S.; Tokura, Y. *Nature* **2001**, *410*, 180.
(9) Allen, P. B.; Perebeinos, V. *Nature* **2001**, *410*, 155.
(10) Ritter, C.; Ibarra, M. R.; De Teresa, J. M.; Algarabel, P. A.; Marquina, C.; Blasco, J.; Garcia, J.; Oseroff, S.; Cheong, S−W. *Phys. Rev. B* **1997**, *56*, 8902.